Transient heat conduction analysis of functionally graded materials by multiple reciprocity boundary face method

Guangyao Li[a], Shuaiping Guo[a], Jianming Zhang[a, b*], Yuan Li[a], Lei Han[a]

[a] State Key Laboratory of Advanced Design and Manufacturing for Vehicle Body, Hunan University, Changsha 410082, China

[b] State Key Laboratory of High Performance Complex Manufacturing, Central South University, Changsha 410083, China

*Correspondence to: Jianming Zhang

College of Mechanical and Vehicle Engineering, Hunan University, Changsha 410082, China

Telephone: +86-731-88823061

E-mail: zhangjm@hnu.edu.cn

Abstract: This paper applies the multiple reciprocity boundary face method to solve transient heat conduction problems of functionally graded materials. It is assumed that the material properties vary in z-direction exponentially or quadratically. Several variable substitutions are employed to convert this problem to standard diffusion equations. After those substitutions, however, the initial condition and the heat source density function, which leads the domain integral of the boundary integral equation, become more complicated. In this application, the Laplace transformation is used to remove the time dependence of the problem. A multiple reciprocity formulation with the modified Helmholtz fundamental solutions is used to convert the domain integral into boundary integrals and several non-integral terms. Numerical examples show that the results of our method are in good agreement with the analytical solutions or finite element method solutions at both internal and boundary points.

Keywords: transient heat conduction, functionally graded materials, boundary face method, Laplace transformation, multiple reciprocity method

1. Introduction

In recent years, functionally graded materials (FGMs) attract great attention in many engineering applications due to its specific characteristic [1]. FGMs are composite materials which merge two or more materials by varying gradually in specific properties such as heat conductivity, specific heat, and density. In this way, it is possible to keep the good properties of all materials. For example, Metal/ceramic FGMs can incorporate advantageous properties of both ceramics and metals such as the heat-resistance of ceramics and the high-hardness of metals. In general, FGMs are often used as structural components in extremely high-temperature environments like applications in aerospace and nuclear reactors. Thus, transient heat conduction analysis is important to the design, optimization and engineering applications of FGMs.

In the past, heat conduction problems in FGMs have been investigated by several researchers. Sutradhar et al. [2] presented the Galerkin BEM with Laplace transform for heat conduction problem in homogeneous and non-homogeneous FGMs. Sladek et al. [3] proposed a meshless method for transient heat conduction analysis in FGMs using local boundary integral equation. Wang et al. [4] developed a virtual boundary collocation method (VBCM) based on Radial Basis Function (RBF) interpolation and

time discretization to analyze this problem. Mirzaei et al [5] presented a new implementation of the meshless local BIE for this problem, in which the moving least squares (MLS) is used for approximating the temperature and heat flux in both time and space domains. Li et al [6] solved the three-dimensional transient heat conduction problems in FGMs using the method of fundamental solutions (MFS). But in these literatures the non-zero initial condition and heat source are not considered. Except the thermal analysis, other physical problems in the FGMs are drawing attention of people, such as frictional contact problems [7] and fracture problems [8].

In this paper, transient heat conduction problems of FGMs considering non-zero initial conditions and arbitrary heat generation are solved by the boundary integral equation (BIE) method [9-13]. We applied the Laplace transformation technology [14] to eliminate the time-dependence of the governing equation. Using the transformation, the parabolic heat conduction equation is converted to a more tractable elliptic equation. Then the boundary integral equation is derived and solved in the Laplace space for a sequence of real positive values of the transform parameter. At last, the inverse transformation is performed to evaluate the physical variables in the real space.

To avoid the domain integration which are related to the initial condition and heat generation in BIE, several methods have been proposed. Tanaka et al. [15] introduced the dual reciprocity method (DRM) to solve the diffusion problem. Nowak and Neves [16] applied the multiple reciprocity method (MRM) to convert the domain integral to an infinite series of boundary integrals using the higher-order fundamental solutions. In the MRM, however, numerical instability was found when the length of time step is small. Based on the MRM, Ochiai and Kitayama [17] proposed a triple reciprocity method. Gao [18] proposed the radial integration method (RIM) to evaluate the domain integrals with boundary-only discretization. In some cases, however, this method still applies internal points for variable interpolation.

The authors found that the fundamental solution of the diffusion governing equation in Laplace space had quickly convergent higher order fundamental solutions. So it is seemly to employ the MRM to convert the domain integrals. The domain integrals will be converted to an infinite series of boundary integrals. And the quickly convergent higher order fundamental solutions make sure that the infinite series can also be computed through several truncated terms. The convergence had been discussed in Reference [19].

In this paper, the Laplace Transformation and Multiple Reciprocity Method (LTMRM) with the modified Helmholtz fundamental solutions will be used to simulate the transient heat conduction in FGMs. The domain integrals will be converted to the boundary integrals successfully. After solving the BIE in Laplace space, the Gaver-Wynn-rho algorithm is applied to transform the solution to the real space [20]. To avoid the geometric errors between the geometric model and the analysis model, our method is implemented in the framework of boundary face method (BFM) program [21-27].

This paper is organized as follows: we introduce the formulation of the BIE in FGMs in Section 2. The MRM in Laplace space are described in detail in Section 3. In Section 4, some numerical examples are shown to verify our method and finally, the paper ends with conclusions in Section 5.

2. Problem definition of transient heat conduction in FGMs

In this section, we will introduce the governing equation, boundary conditions and initial condition of transient heat conduction problem in FGMs. A brief review will be given on how to convert the general transient diffusion equation to a standard diffusion equation [2].

The transient heat conduction problem can be represented as:

$$\nabla \cdot (k\nabla\phi) = c\rho\frac{\partial\phi}{\partial t} - h(\mathbf{Q},t) \qquad (\mathbf{Q}\in\Omega) \tag{1}$$

where $\phi = \phi(\mathbf{Q},t)$ is the temperature of the location **Q** at the time *t*. The coefficients *k*, *c* and ρ are the heat conductivity, the specific heat and the density, respectively. The function *h(***Q***, t)* is the heat source density. Ω stands for the considered domain enclosed by $\Gamma_1 U\, \Gamma_2$. The boundary conditions are given as the following types:

$$\begin{aligned} \phi(\mathbf{Q},t) &= \bar{\phi}(\mathbf{Q},t), \qquad \mathbf{Q}\in\Gamma_1 \\ q(\mathbf{Q},t) &= \frac{\partial\phi(\mathbf{Q},t)}{\partial\mathbf{n}}, \qquad \mathbf{Q}\in\Gamma_2 \end{aligned} \tag{2}$$

in which $\bar{\phi}, \partial\phi/\partial\mathbf{n}$ stand for the prescribed temperature and normal flux on the boundary respectively. And **n** is the unit outward normal to Γ_2. The initial conditions at time $t=t_0$ can be prescribed as

$$\phi_0(\mathbf{Q}) = \phi(\mathbf{Q},t_0), \quad \mathbf{Q}\in\Omega \tag{3}$$

If the heat conductivity and the specific heat have the same functional variation, say e.g.,

$$k(x,y,z) = k_0 f(x,y,z) \tag{4}$$

and

$$c(x,y,z) = c_0 f(x,y,z) \tag{5}$$

respectively then by introducing variable substitution, Eq. (1) can be transformed into the standard diffusion equation.

2.1 Exponential variations

In the first case, we assume that the thermal conductivity and the specific heat of the FGMs vary exponentially in the z-direction, i.e.

$$k(x,y,z) = k(z) = k_0 e^{2\beta z} \tag{6}$$

$$c(x,y,z) = c(z) = c_0 e^{2\beta z} \tag{7}$$

where β is the material non-homogeneous parameter.

Substituting these material expressions in Eq. (4) and Eq. (5) into Eq. (1), we obtain

$$\frac{\partial\phi}{\partial t} = \alpha\left(\nabla^2\phi + 2\beta\phi_z\right) + \frac{1}{c\rho}h(\mathbf{Q},t) \tag{8}$$

where $\alpha=k_0/(c_0\rho)$ is the thermal diffusivity and $\phi_z = \partial\phi/\partial z$. If the following substitution is employed

$$\phi = e^{-\beta z-\beta^2\alpha t}\times u \tag{9}$$

Eq. (8) will be converted to

$$\frac{\partial u}{\partial t} = \alpha\nabla^2 u + \frac{1}{c\rho}\tilde{h}(\mathbf{Q},t) \tag{10}$$

which is the standard diffusion equation for a homogeneous material problem. We denote for short

$$\tilde{h}(\mathbf{Q},t) = h(\mathbf{Q},t)\times e^{\beta z+\beta^2\alpha t} \tag{11}$$

And the initial condition is

$$u_0 = \phi_0 \times e^{\beta z+\beta^2\alpha t} \tag{12}$$

The boundary conditions for Eq. (8) are

$$\begin{aligned} u(\mathbf{Q},t) &= \bar{\phi}(\mathbf{Q},t)\times e^{\beta z+\beta^2\alpha t}, \quad \mathbf{Q}\in\Gamma_1 \\ q(\mathbf{Q},t) &= \frac{\partial u(\mathbf{Q},t)}{\partial \mathbf{n}} = \frac{\partial \phi(\mathbf{Q},t)}{\partial \mathbf{n}}\times e^{\beta z+\beta^2\alpha t} + \bar{\phi}(\mathbf{Q},t)\times e^{\beta z+\beta^2\alpha t}\beta n_z, \quad \mathbf{Q}\in\Gamma_2 \end{aligned} \tag{13}$$

2.2 Quadratic variations

In the second case, we assume that the thermal conductivity and the specific heat of the FGMs vary quadratically in the z-direction as the following functions:

$$k(x,y,z) = k(z) = k_0(a_1 + a_2 z)^2 \tag{14}$$

$$c(x,y,z) = c(z) = c_0(a_1 + a_2 z)^2 \tag{15}$$

where a_1 and a_2 are arbitrary constants.

If substituting the formulation

$$\phi = \frac{1}{\sqrt{k(z)}}\times u \tag{16}$$

into Eq. (1), the Eq. (1) will be converted to the standard diffusion equation as Eq. (8). The corresponding formulation of $\tilde{h}(\mathbf{Q},t)$ in Eq. (8) is

$$\tilde{h}(\mathbf{Q},t) = h(\mathbf{Q},t)\times\sqrt{k(z)} = \sqrt{k_0}(a_1 + a_2 z)\times h(\mathbf{Q},t) \tag{17}$$

and initial condition is

$$u_0 = \phi_0\times\sqrt{k(z)} = \sqrt{k_0}(a_1 + a_2 z)\times\phi_0 \tag{18}$$

The boundary conditions for Eq. (8) in this case are

$$\begin{aligned} u(\mathbf{Q},t) &= \bar{\phi}(\mathbf{Q},t)\times\sqrt{k(z)}, \quad \mathbf{Q}\in\Gamma_1 \\ q(\mathbf{Q},t) &= \frac{\partial u(\mathbf{Q},t)}{\partial \mathbf{n}} = \frac{\partial \phi(\mathbf{Q},t)}{\partial \mathbf{n}}\sqrt{k(z)} + \bar{\phi}(\mathbf{Q},t)\frac{1}{2\sqrt{k(z)}}\frac{\partial k(z)}{\partial z}n_z, \quad \mathbf{Q}\in\Gamma_2 \end{aligned} \tag{19}$$

From the above two cases, it can be concluded that if we can find some functions which meet the conversion request, the standard diffusion equation can be obtained. In the following two cases, the FGM transient problem also can be transformed into a standard diffusion problem.

- If $k(x, y, z)$ and $c(x, y, z)$ vary with z as functions

$$k(x,y,z) = k(z) = k_0(a_1 e^{\beta z} + a_2 e^{-\beta z})^2 \tag{20}$$

$$c(x,y,z) = c(z) = c_0(a_1 e^{\beta z} + a_2 e^{-\beta z})^2 \tag{21}$$

the following substitution can be employed

$$\phi = \frac{1}{\sqrt{k(z)}}e^{-\beta^2\alpha}\times u \tag{22}$$

- If $k(x, y, z)$ and $c(x, y, z)$ vary with z as functions

$$k(x,y,z) = k(z) = k_0(a_1\cos\beta z + a_2\sin\beta z)^2 \tag{23}$$

$$c(x,y,z) = c(z) = c_0(a_1\cos\beta z + a_2\sin\beta z)^2 \tag{24}$$

the following substitution can be employed

$$\phi = \frac{1}{\sqrt{k(z)}} e^{\beta^2 \alpha} \times u \tag{25}$$

3. Numerical implementation

In this section, we will briefly introduce the boundary integral equation in Laplace space for the above problem. The MRM with the quickly convergent higher order fundamental solutions will be used to convert the domain integrals to boundary integrals [19].

We denote the Laplace transform (LT) of a function $u(\mathbf{Q}, t)$ by

$$\tilde{u}(\mathbf{Q}, s) = \int_0^\infty u(\mathbf{Q}, t) e^{-st} dt \tag{26}$$

where s is the transform parameter. The heat source function in Eq. (11) after LT is

$$h(\mathbf{Q}, s) = \int_0^\infty h(\mathbf{Q}, t) \times e^{\beta z + \beta^2 \alpha t} e^{-st} dt = e^{\beta z} \int_0^\infty h(\mathbf{Q}, t) \times e^{-(s - \beta^2 \alpha)t} dt = e^{\beta z} \tilde{h}(\mathbf{Q}, s - \beta^2 \alpha) \tag{27}$$

and the heat source function in Eq. (17) after LT is

$$h(\mathbf{Q}, s) = \int_0^\infty h(\mathbf{Q}, t) \times \sqrt{k(z)} e^{-st} dt = \sqrt{k(z)} \int_0^\infty h(\mathbf{Q}, t) e^{-st} dt = \sqrt{k(z)} \times \tilde{h}(\mathbf{Q}, s) \tag{28}$$

Implementing the LT on Eq. (10), we have the following governing equation:

$$\nabla^2 \tilde{u} - \lambda \tilde{u} = -\frac{1}{\alpha} u_0 - \frac{1}{k_0} h(\mathbf{Q}, s) \tag{29}$$

where $\lambda = s/\alpha$ and u_0 is the initial condition at time $t = t_0$. It is worth noting that this is actually a modified Helmholtz equation. The fundamental solutions of the Eq. (29) are

$$\begin{aligned} u^* &= \frac{-1}{4\pi r} e^{-\sqrt{\lambda} r} \\ q^* &= \frac{\partial u^*}{\partial \mathbf{n}} = \frac{1}{4\pi r^2} (1 + \sqrt{\lambda} r) e^{-\sqrt{\lambda} r} \frac{\partial r}{\partial \mathbf{n}} \end{aligned} \tag{30}$$

which satisfy the following equation:

$$\nabla^2 u^* - \lambda u^* = \Delta(\mathbf{Y}, \mathbf{Q}) \tag{31}$$

in which $\mathbf{Y}$ represents the source point belong Ω, $\Delta(x, y)$ is the Dirichlet function. By employing the fundamental solutions in Eq. (30), Eq. (29) can be converted into the following BIE:

$$\int_\Gamma q^* \tilde{u} d\Gamma - c\tilde{u}(\mathbf{Y}) - \int_\Gamma u^* \tilde{q} d\Gamma = \frac{1}{\alpha} \int_\Omega u^* b(\mathbf{Q}, s) d\Omega \tag{32}$$

where the value of the constant c is

$$c = \begin{cases} 0 & \mathbf{Y} \in \bar{\Omega} \\ 1 & \mathbf{Y} \in \Omega \\ 0.5 & \mathbf{Y} \in \Gamma_1 \bigcup \Gamma_2 \end{cases} \tag{33}$$

We denote for short

$$b(\mathbf{Q}, s) = \frac{1}{\alpha} u_0 + \frac{1}{k_0} h(\mathbf{Q}, s) \tag{34}$$

A sequence of higher order fundamental solutions can be defined by the recurrence formula

$$
\begin{aligned}
&u^{*(0)} = u^* \\
&\nabla^2 u^{*(j+1)} = u^{*(j)}, \quad (j = 0,1,2,\cdots) \\
&q^{*(j+1)} = \frac{\partial u^{*(j+1)}}{\partial \mathbf{n}}
\end{aligned} \tag{35}
$$

or by the formula

$$
\begin{aligned}
&u^{*(j)} = (1/\lambda^j) u^{*(0)}, \quad (j = 0,1,2,\cdots) \\
&q^{*(j)} = (1/\lambda^j) q^{*(0)}
\end{aligned} \tag{36}
$$

The higher order source functions and higher order initial conditions are listed as follows:

$$
\begin{aligned}
&h^{(0)} = h, \quad h^{(j)} = \nabla^2 h^{(j-1)}, \qquad (j = 1,2,3,\cdots), \\
&u_0^{(0)} = u_0, \quad u_0^{(j)} = \nabla^2 u_0^{(j-1)}, \qquad (j = 1,2,3,\cdots).
\end{aligned} \tag{37}
$$

and

$$
\begin{aligned}
b^{(0)} &= \frac{1}{\alpha} u_0 + \frac{1}{k_0} h^{(0)} \\
b^{(j)} &= \frac{1}{\alpha} u_0^{j(\ )} + \frac{1}{k_0} h^{j(\ )} \\
b_n^{(j)} &= \frac{\partial b^{(j)}}{\partial \mathbf{n}} = \frac{1}{\alpha} \frac{\partial u_0^{(j)}}{\partial \mathbf{n}} + \frac{1}{k_0} \frac{\partial h^{(j)}}{\partial \mathbf{n}}
\end{aligned} \tag{38}
$$

Considering Eq. (35), we reform Eq. (31) into the following equation:

$$
u^{*(0)} = \frac{1}{\lambda} \nabla^2 u^* + \frac{1}{\lambda} \Delta(\mathbf{Y}, \mathbf{Q}) = \frac{1}{\lambda} u^{*(1)} + \frac{1}{\lambda} \Delta(\mathbf{Y}, \mathbf{Q}) \tag{39}
$$

Using reciprocity scheme, the domain integral can be represented recursively by:

$$
\begin{aligned}
\int_\Omega u^{*(0)} b^{(0)} d\Omega &= \int_\Omega \left(\frac{1}{\lambda} \nabla^2 u^* - \frac{1}{\lambda} \Delta(\mathbf{Y}, \mathbf{Q}) \right) b^{(0)} d\Omega \\
&= \int_\Omega \frac{1}{\lambda} u^* b^{(1)} d\Omega + \int_\Gamma q^* \frac{1}{\lambda} b^{(0)} d\Gamma - \int_\Gamma u^* \frac{1}{\lambda} b_n^{(0)} d\Gamma - c \frac{1}{\lambda} b^{(0)}(\mathbf{Y}) \\
&= \int_\Gamma q^* \sum_{j=0}^{\infty} \frac{1}{\lambda^{j+1}} b^{(j)} d\Gamma - \int_\Gamma u^* \sum_{j=0}^{\infty} \frac{1}{\lambda^{j+1}} b_n^{(j)} d\Gamma - c \sum_{j=0}^{\infty} \frac{1}{\lambda^{j+1}} b^{(j)}(\mathbf{Y}) \\
&\approx \int_\Gamma q^* \sum_{j=0}^{M-1} \frac{1}{\lambda^{j+1}} b^{(j)} d\Gamma - \int_\Gamma u^* \sum_{j=0}^{M-1} \frac{1}{\lambda^{j+1}} b_n^{(j)} d\Gamma - c \sum_{j=0}^{M-1} \frac{1}{\lambda^{j+1}} b^{(j)}(\mathbf{Y})
\end{aligned} \tag{40}
$$

where the value of the constant c is shown in Eq. (33).

If the function $b(\mathbf{Q}, s)$ can be expressed by a polynomial function, $b^{(j)}$ and $b_n^{(j)}$ approach to zero with an increasing j. Thus the infinite series of boundary integrals will become finite exactly. If the function $b(\mathbf{Q}, s)$ is more general, bearing in mind the convergence of the higher order fundamental solution that had been discussed in Reference [19], the infinite series can also be computed through several truncated terms.

Discretization of the boundary Γ into boundary elements allows one to replace the integrals in Eq. (32) by the summation of integrals, each one along particular boundary element Γ_n

$$
\begin{aligned}
&\sum_{n=1}^{N} \int_{\Gamma_n} q^* \tilde{u} d\Gamma_n - c_i \tilde{u}(Y) - \sum_{n=1}^{N} \int_{\Gamma_n} u^* \tilde{q} d\Gamma_n \\
&= \frac{1}{\alpha} \sum_{n=1}^{N} \left(\int_{\Gamma_n} q^* \sum_{j=0}^{M-1} \frac{1}{\lambda^{j+1}} b^{(j)} d\Gamma_n - \int_{\Gamma_n} u^* \sum_{j=0}^{M-1} \frac{1}{\lambda^{j+1}} b_n^{(j)} d\Gamma_n \right) - \frac{c}{\alpha} \sum_{j=0}^{M-1} \frac{1}{\lambda^{j+1}} b^{(j)}(\mathbf{Y})
\end{aligned} \tag{41}
$$

In this paper, the BFM is used to implement the boundary integrations in Eq. (41). It should be mentioned that the BFM is implemented directly based on the boundary representation data structure (B-rep) that is used in most CAD packages for geometry modeling. Each bounding surface of geometry model is represented as parametric form by the geometric map between the parametric space and the physical space. Both boundary integration and variable approximation are performed in the parametric space. The integrand quantities are calculated directly from the faces rather than from elements, and thus no geometric error will be introduced. In Fig. 1, a cylinder is discretized with BFM and BEM respectively. It can be seen that the mesh of BEM simulates the geometry of cylinder approximately, while the mesh of BFM expresses the geometry exactly. The details of the implementation for the BFM can be found in Refs. [21, 22].

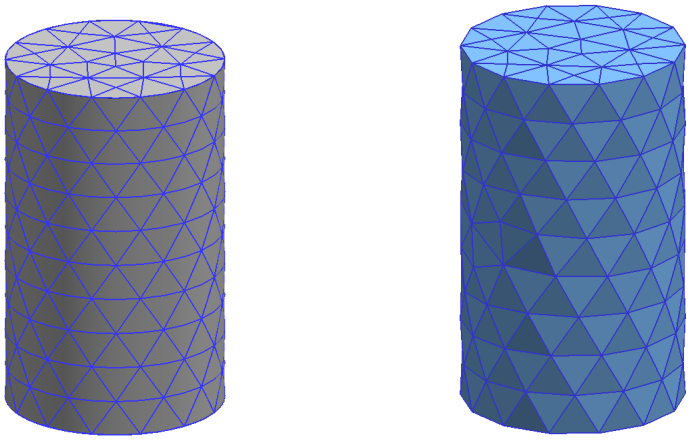

(a) BFM (b) BEM

Figure 1: Discretized models of a cylinder with BFM and BEM.

Finally, we collocate the field points at all interpolation points and the following system is obtained

$$\mathbf{HU}-\mathbf{GQ}=\mathbf{R} \tag{42}$$

where the entries of the matrices are

$$\begin{aligned}
&\mathbf{H}=\mathbf{H}^0-0.5\mathbf{I} \quad \mathbf{G}=\mathbf{G}^0\\
&\mathbf{R}=\frac{1}{\alpha}\sum_{j=0}^{M-1}\left(\mathbf{H}^{j+1}\mathbf{B}^j-\mathbf{G}^{j+1}\mathbf{B}_n^j\right)=\frac{1}{\alpha}\mathbf{H}\sum_{j=0}^{M-1}\frac{1}{\lambda^{j+1}}\mathbf{B}^j-\frac{1}{\alpha}\mathbf{G}\sum_{j=0}^{M-1}\frac{1}{\lambda^{j+1}}\mathbf{B}_n^j\\
&H_{ij}^0=\int_{\Gamma_j}\Psi^T q^* d\Gamma_j\,,\quad H_{ij}^k=\int_{\Gamma_j}\Psi^T q^{*(k)} d\Gamma_j=\frac{1}{\lambda^k}H_{ij}^0\\
&G_{ij}^0=\int_{\Gamma_j}\Psi^T u^* d\Gamma_j\,,\quad G_{ij}^k=\int_{\Gamma_j}\Psi^T u^{*(k)} d\Gamma_j=\frac{1}{\lambda^k}G_{ij}^0
\end{aligned} \tag{43}$$

in which the function Ψ is the shape function in each element.

Firstly, the numerical solution in Laplace space should be transferred into the time space by the Laplace inversion. The inversion formula used in this paper is Gaver functionals [28]. And the Wynn's rho algorithm is employed to increase the accuracy of the approximant [29]. After obtaining the solutions in time space, we substitute them into Eq. (9) or (16) to get the real solutions for FGMs problems.

4. Numerical examples

In this section, solutions for three transient heat conduction problems in FGMs are presented. The first one considers a cube of FGMs which material properties such as thermal conductivity and the

specific heat are varying exponentially. This example verifies the accuracy of the governing equation derived in Section 2. The second one considers a cube of FGMs with quadratic heat source density, which becomes exponential heat source density after using the substitution in Eq. (9), to demonstrate the accuracy and convergence of the modified MRM presented in Section 3. The last example analyzes a FGMs sphere with quadratic initial condition. The thermal conductivity and the specific heat in this example are varying quadratically.

4.1 A FGMs cube with constant temperature on two faces

In the first example, we consider a unit cube of FGMs with zero initial temperature. Then the cube is suddenly heated on the top face such that a temperature of 100℃ is maintained for *t>0*. Meanwhile the temperature of the bottom face is 0℃. The remaining four faces are insulated (zero normal flux). The geometry and the boundary conditions are shown in Fig. 2.

The thermal conductivity and the specific heat of FGMs are taken to be

$$k(x,y,z)=k_0e^{2\beta z}\ \mathrm{W}/(\mathrm{m}\cdot\mathrm{k}) \tag{44}$$

$$c(x,y,z)=c_0e^{2\beta z}\ \mathrm{J}/(\mathrm{kg}\cdot\mathrm{k}) \tag{45}$$

And the density $\rho=1\mathrm{kg}/\mathrm{m}^3$.

In this example, in order to study the effect of different FGMs on the behavior of heat transfer, we adopt $\beta=1.5,0,-1.5$ respectively to observe the results. The analytical solution for temperature of this problem is given by

$$\begin{aligned}\phi(x,y,z;t)&=T\frac{1-e^{-2\beta z}}{1-e^{-2\beta L}}+\sum_{n=1}^{\infty}B_n\sin\frac{n\pi z}{L}e^{-\beta z}e^{-(n^2\pi^2/L^2+\beta^2)\alpha t}\\ B_n&=\frac{2Te^{\beta L}n\pi\cos(n\pi)}{\beta^2L^2+n^2\pi^2}\end{aligned} \tag{46}$$

where *L* is the dimension of the cube (in the z-direction). The surfaces of the cube are discretized with 150 boundary linear quadrilateral elements and 216 nodes.

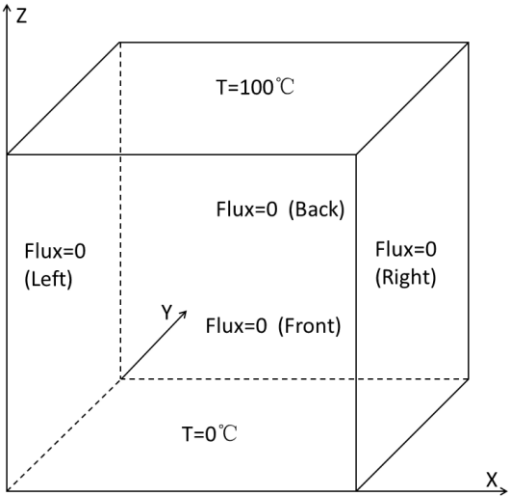

Figure 2: Geometry and boundary conditions of a cube.

Fig. 3, Fig. 4 and Fig. 5 show the time evolution of the temperature at points along the z-axis at *z=0.2, 0.4, 0.6, 0.8* when $\beta=1.5,0,-1.5$ respectively. As we can see, all of the temperature variation matches the analytical solution very well. When $\beta=0$, the material becomes homogeneous and the

temperature distributes linearly. When $\beta = 1.5$, higher temperature is obtained at the same points compared with the case of $\beta = 0$ due to the larger thermal conductivity. And the distribution varies exponentially. When $\beta = -1.5$, lower temperature is obtained compared with the case of $\beta = 0$. In this case, the distribution also varies exponentially. From these three pictures, difference between the homogeneous material and the FGMs can be observed.

The solution of flux on the bottom when $\beta = 1.5$ is shown in Fig. 6, which is also in a good agreement with the analytical solution. From these pictures, it is verified that the FGMs problems can be well simulated by the boundary face method using the fundamental solutions of standard diffusion problem directly.

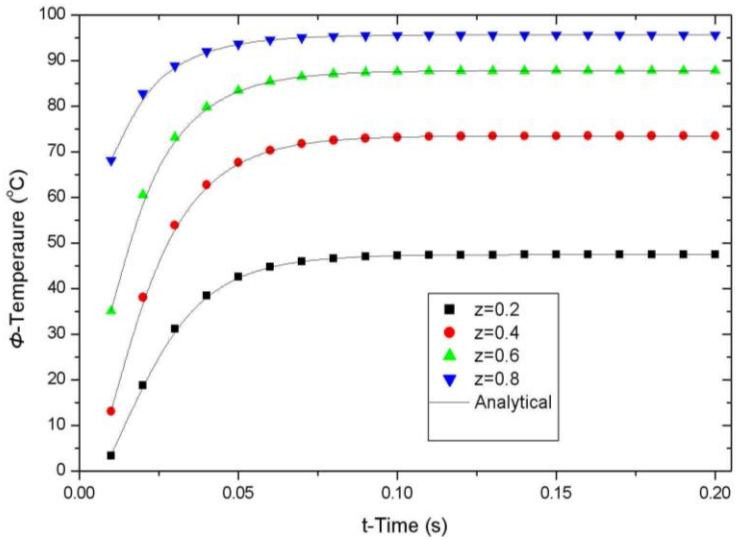

Figure 3: Temperature variation history of several points along the z-direction: $\beta = 1.5$.

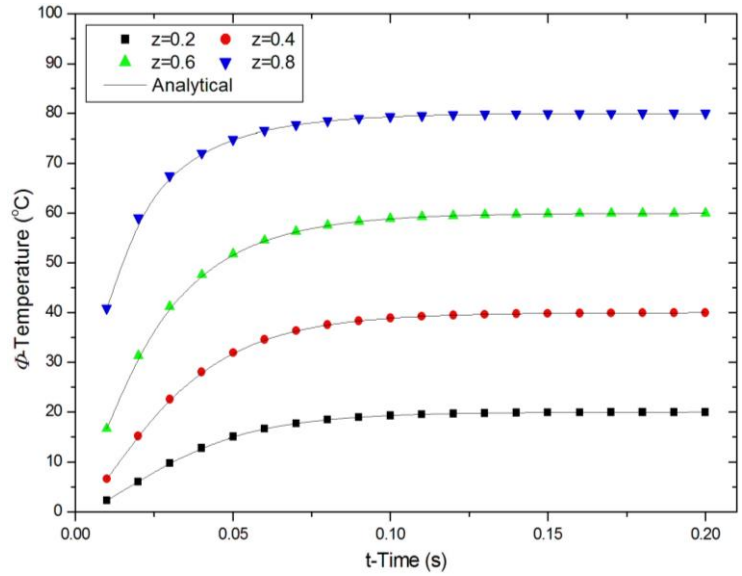

Figure 4: Temperature variation history of several points along the z-direction: $\beta = 0$.

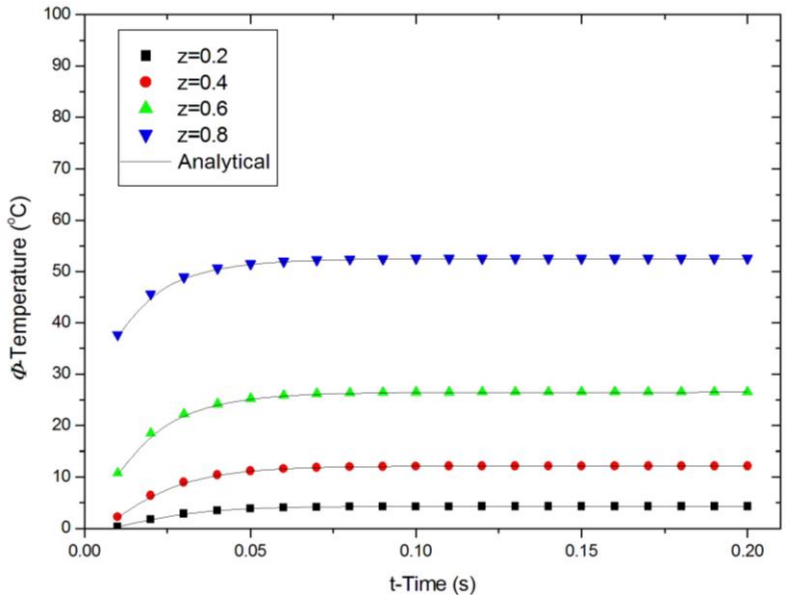

Figure 5: Temperature variation history of several points along the z-direction: $\beta = -1.5$.

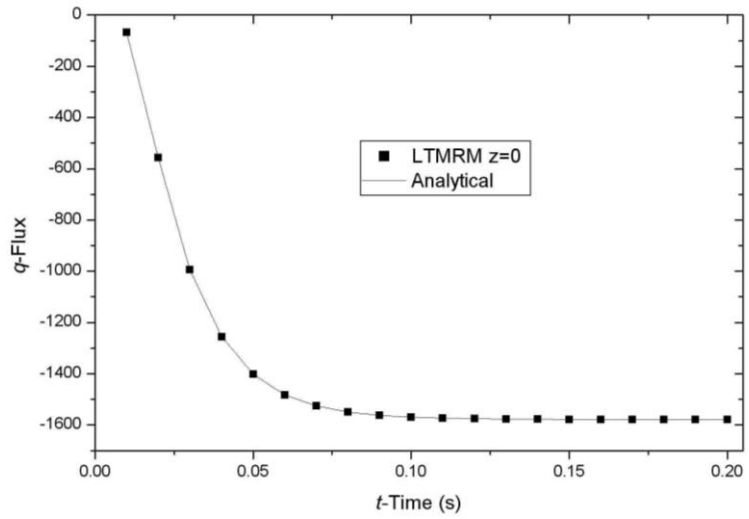

Figure 6: Flux variation history on the bottom face: $\beta = 1.5$.

4.2 A FGMs cube with quadratic heat source density

In this example we analyze a cube with heat generation. As shown in Fig. 7, the top surface and bottom surface of the cube is maintained at a temperature of *T=0* ℃. The remaining four faces are insulated (zero normal flux). The edge length of the cube is *L=1m*. The thermal conductivity, the specific heat and the density are taken to be

$$k(x,y,z) = k_0 e^{2\beta z} = 40e^{20z}\ \mathrm{W}/(\mathrm{m}\cdot\mathrm{k}) \tag{47}$$

$$c(x,y,z) = c_0 e^{2\beta z} = 500e^{20z}\ \mathrm{J}/(\mathrm{kg}\cdot\mathrm{k}) \tag{48}$$

$$\rho = 8000\,\mathrm{kg}/\mathrm{m}^3 \tag{49}$$

The heat generation is given by

$$h(\mathbf{Q},t) = x^2 + y \tag{50}$$

After using the substitution in Eq. (9), the heat density function in the diffusion equation becomes

$$\tilde{h}(\mathbf{Q},t) = h(\mathbf{Q},t) \times e^{\beta z + \beta^2 \alpha t} = (x^2 + y)e^{10z + 0.001t} . \tag{51}$$

After Laplace transform, the heat density function is represented by

$$h(\mathbf{Q},s) = (x^2 + y)\frac{e^{\beta z}}{s - \beta^2 \alpha} = \frac{(x^2 + y)e^{10z}}{s - 0.001} . \tag{52}$$

The high order derivatives of it are:

$$\begin{aligned} h^{(0)}(\mathbf{Q},s) &= h(\mathbf{Q},s) = \frac{(x^2 + y)e^{10z}}{s - 0.001} \\ h^{(1)}(\mathbf{Q},s) &= \frac{100(x^2 + y)e^{10z} + 2e^{10z}}{s - 0.001} \\ h^{(2)}(\mathbf{Q},s) &= \frac{10000(x^2 + y)e^{10z} + 400e^{10z}}{s - 0.001} \end{aligned} \tag{53}$$

Obviously, the values of the higher order heat source functions are not convergent. The growth rate of $h^{(j)}$ in eq. (53) is less than 200. The growth rate of the high order fundamental solutions $u^{*(j)}$ in eq. (36) is $1/\lambda = \alpha / s$. In this example the thermal diffusivity α=1.0e-5. The coefficient s is determined by the Laplace inversion formula and the time variable t. Its order of magnitude is -2 in this simulation. Therefore the growth rate of $u^{*(j)}$ is about 1.0e-3. Comparing the growth rate of $h^{(j)}$ and $u^{*(j)}$ it can be concluded that the high order fundamental solutions converge quickly enough to guarantee the accuracy of MRM.

In this analysis, 150 boundary quadratic quadrilateral elements and 576 boundary nodes are used. Fig. 8 shows the time evolution of the temperature at different points in domain. It is worth to observe that our results are in excellent agreement with the results obtained from Abaqus which is software based on the finite element method. Fig. 9 and Fig. 10 present the temperature distribution of model at time *t=50s* and *t=100s* respectively. They coincide with the distribution of heat density given. This example demonstrates that using the MRM with the quickly convergent higher order fundamental solutions in our method, the FGMs problem with heat generation can be solved accurately and efficiently.

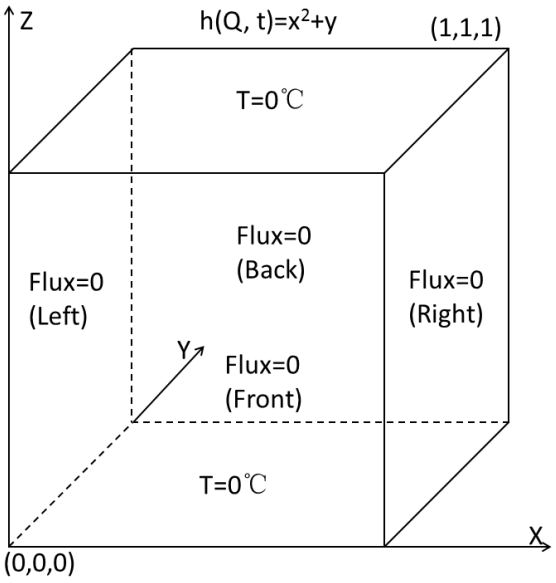

Figure 7: Geometry and boundary conditions of the FGMs cube with heat generation.

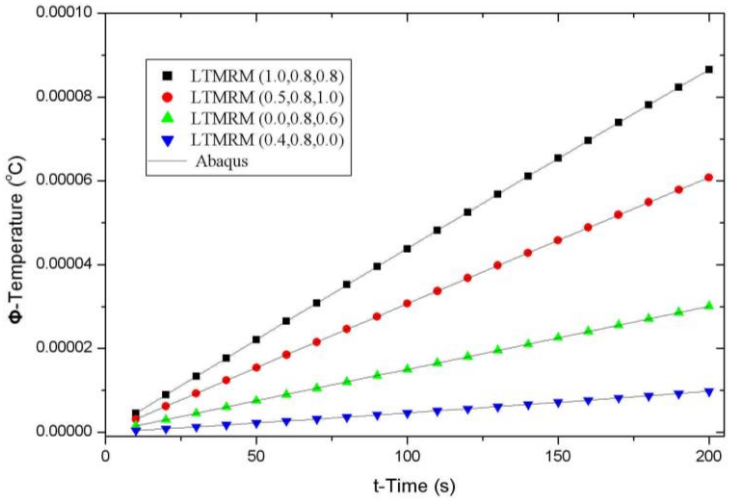

Figure 8: Temperature variation history of several internal points.

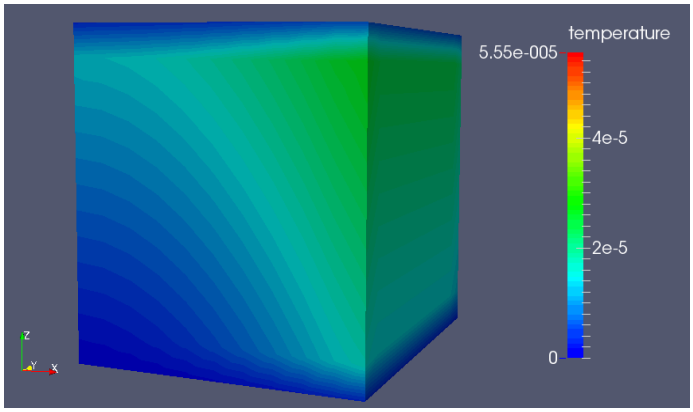

Figure 9: Temperature distribution at time *t=50s*.

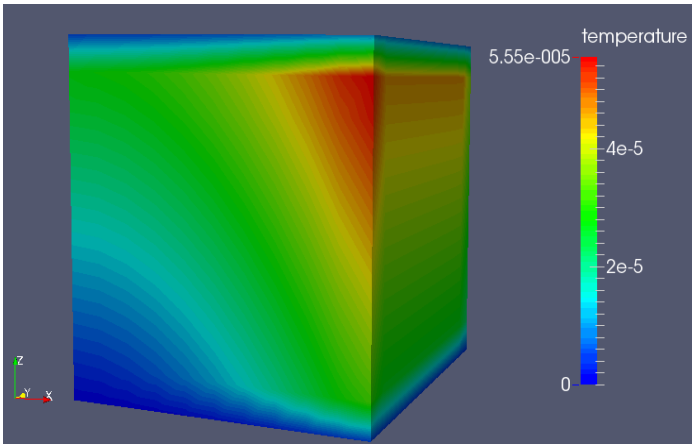

Figure 10: Temperature distribution at time *t=100s*.

4.3 A FGMs sphere with initial temperature

In this example we consider a FGMs sphere with initial temperature. Different with the above two examples, the thermal conductivity and the specific heat of this model are varying quadratically in the

z-direction as the following functions:

$$k(x,y,z)=k_0(a_1+a_2z)^2=900\left(2+z\right)^2\ \mathrm{W}/\left(\mathrm{m}\cdot\mathrm{k}\right) \tag{54}$$

$$c(x,y,z)=c_0(a_1+a_2z)^2=40\left(2+z\right)^2\ \mathrm{J}/\left(\mathrm{kg}\cdot\mathrm{k}\right) \tag{55}$$

The density is given

$$\rho=1000\mathrm{kg}/\mathrm{m}^3 \tag{56}$$

Fig. 11 shows the geometry and the mesh of the sphere. The radius is 1m. We discretize the model with 160 linear quadrilaterals and 40 triangles. The node number is 231.

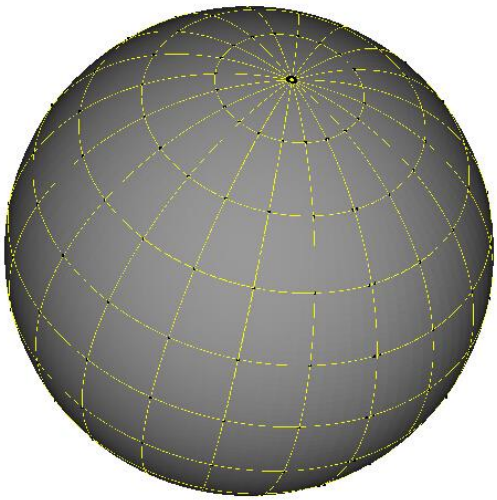

Figure 11: Discretized model of shpere.

At the beginning of analysis, initial temperature is given as follows:

$$\phi_0=100\left(1-x^2-y^2-z^2\right) \tag{57}$$

After using the substitution in Eq. (15), the function of initial temperature in the diffusion equation becomes

$$u_0=3000\left(1-x^2-y^2-z^2\right)\left(2+z\right) \tag{58}$$

High order functions of it are:

$$\begin{aligned} u_0^{(0)}(\mathbf{Q})&=3000\left(1-x^2-y^2-z^2\right)\left(2+z\right)\\ u_0^{(1)}(\mathbf{Q})&=3000\left(-12-10z\right)\\ u_0^{(2)}(\mathbf{Q})&=0.0 \end{aligned} \tag{59}$$

It can be observed that the high order initial temperature functions are convergent naturally. In this case, the domain integrals can be analytically converted to boundary integrals through several reciprocal procedures.

In this analysis, the temperature of the surface of sphere is maintained 0℃ for $t>0$. Fig. 12 shows the comparison between the numerical solutions and the FEM solutions which is solved by Abaqus software at t=0, 2, 6, 12 and 24s. The evaluated points are evenly distributed along the center line of z-direction from (0, 0, -1) to (0, 0, 1). Fig. 13 shows the time evolution of the flux at surface point (0, 0, 1) and (0, 0, -1). It can be seen from these two figures that our results are excellent agreement with the

FEM results, demonstrating the high accuracy of the method proposed in this paper again.

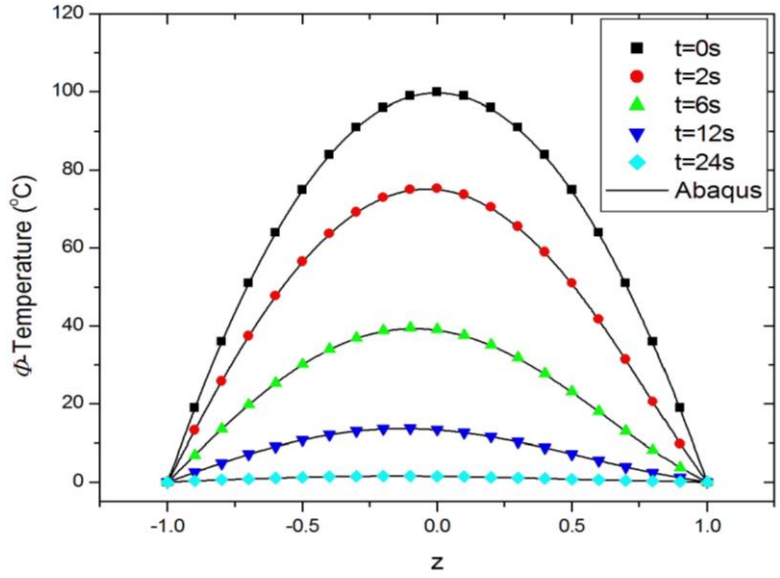

Figure 12: Temperature distribution along the center line of *z*-direction.

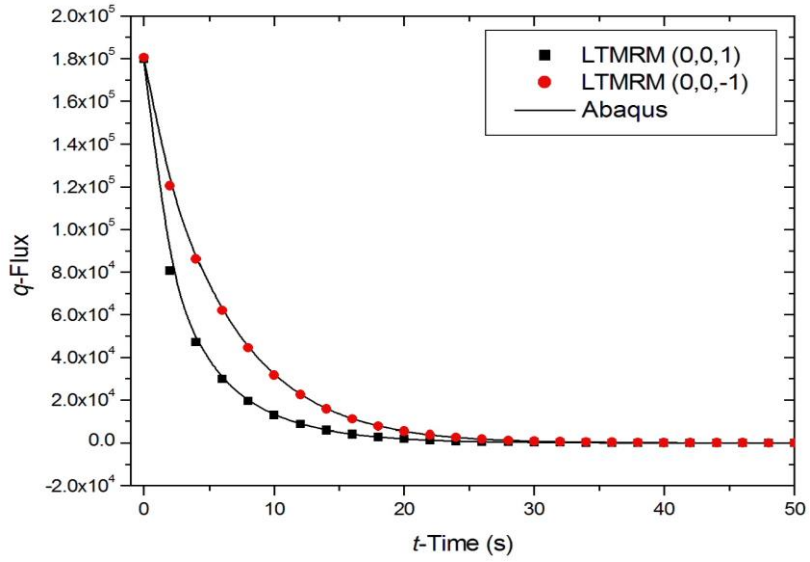

Figure 13: Flux variation history on two points.

5. Conclusion

Three-Dimension transient heat conduction problems in FGMs with heat generation are solved by the BFM which combines the Laplace transformation and the multiple reciprocity method. The general transient diffusion equations for FGMs with material properties which are vary exponentially or quadratically in the *z*-direction are converted to a standard diffusion equation. The domain integrals related to the heat generation and initial condition are converted to boundary integrals successfully by the multiple reciprocity formulation. Numerical results illustrate the accuracy of the proposed method.

In our method, with the quickly convergent higher order fundamental solutions, most of the domain integrals, which appear in the BIE of transient heat conduction problem in FGMs, can be converted to several boundary integrals and non-integral terms. Furthermore, due to the simple form of

the higher order fundamental solutions in our method, the implementation of our method is very simple and no additional matrix is required even for a large number of orders of the fundamental solutions. With the help of the Gaver-Wynn-rho formulation, we computed the inverse Laplace transformation accurately and efficiently in our implementation.

Acknowledgement

This work was supported in part by National Science Foundation of China (Grant No. 11172098 and No. 11472102) and in part by Open Research Fund of Key Laboratory of High Performance Complex Manufacturing, Central South University (Grant No. Kfkt2013-05).

References

[1] Suresh S, Mortensen A. Fundamentals of functionally graded materials. London: IOM Communications Ltd.; 1998.

[2] Sutradhar A, Paulino GH. The simple boundary element method for transient heat conduction in functionally graded materials. Comput Method Appl M 2004; 193: 4511-4539.

[3] Sladek J, Sladek V, Zhang C. Transient heat conduction analysis in functionally graded materials by the meshless local boundary integral equation method. Com Mater Sci 2003; 28: 494-504.

[4] Wang H, Qin QH, Kang YL. A meshless model for transient heat conduction in functionally graded materials. Comput Mech 2006; 38(1): 51-60.

[5] Mirzaei D, Dehghan M. New implementation of MLBIE method for heat conduction analysis in functionally graded materials. Eng Anal Bound Elem 2012; 36: 511-519.

[6] Li M, Chen CS, Chu CC, Young DL. Transient 3D heat conduction in functionally graded materials by the method of fundamental solutions. Eng Anal Bound Elem 2014; 45: 62-67.

[7] Gun H, Gao XW. Analysis of frictional contact problems for functionally graded materials using BEM. Eng Anal Bound Elem 2014; 38: 1-7.

[8] Gao XW, Zhang C, Sladek J, Sladek V. Fracture analysis of functionally graded materials by a BEM. Compos Sci Technol 2008; 68: 1209-1215.

[9] Brebbia CA, Telles JCF, Wrobel LC. Boundary Element Techniques-theory and applications in engineering. Berlin: Springer; 1984.

[10] Cheng AHD, Cheng DT. Heritage and early history of the boundary element method. Eng Anal Bound Elem 2005; 29: 268-302.

[11] Chen JT, Lin SR, Chen KH. Degenerate scale problem when solving Laplaces equation by BEM and its treatment. Int J Numer Methods Eng 2005; 62(2): 233-261.

[12] Liu YJ, Mukherjee S, Nishimura N, Schanz M, Ye W, Sutradhar A, Pan E, Dumont NA, Frangi A, Saez A. Recent advances and emerging applications of the boundary element method. Appl Mech Rev 2011; 64: 030802.

[13] Wang HT, Yao ZH. Large-scale thermal analysis of fiber composites using a line-inclusion model by the fast boundary element method. Eng Anal Bound Elem 2013; 37(2): 319-326.

[14] Rizzo FJ, Shippy DJ. A method of solution for certain problems of transient heat conduction. AIAA J 1970; 8(11): 2004-2009.

[15] Tanaka M, Matsumoto T, Takakuwa S. Dual reciprocity BEM based on time-stepping scheme for the solution of transient heat conduction problems. International Series on Advances in Boundary Elements, Boundary elements XXV 2002; 299-308.

[16]Nowak AJ, Neves AC. The multiple reciprocity boundary element method. Springer; 1994; 45-67.

[17]Ochiai Y, Kitayama Y. Three-dimensional unsteady heat conduction analysis by triple-reciprocity boundary element method. Eng Anal Bound Elem 2009; 33(6): 789-795.

[18]Gao XW. The radial integration method for evaluation of domain integrals. Eng Anal Bound Elem 2002; 26: 905-916.

[19]Guo SP, Zhang JM, Li GY, Zhou FL. Three dimensional transient heat conduction analysis by Laplace transformation and multiple reciprocity boundary face method. Eng Anal Bound Elem 2013; 37(2): 15-22.

[20]Abate J, Valko, PP. Multi-precision Laplace transform inversion. Int J Numer Methods Eng 2004; 60(5): 979-993.

[21]Zhang JM, Qin XY, Han X, Li GY. A boundary face method for potential problems in three dimensions. Int J Numer Methods Eng 2009; 80(3): 320-337.

[22] Qin XY, Zhang JM, Li GY, Sheng XM, Song M, Mu DH. An element implementation of the boundary face method for 3D potential problems. Eng Anal Bound Elem 2010; 34: 934-943.

[23]Zhou FL, Xie GZ, Zhang JM, Zheng XS. Transient heat conduction analysis of solids with small open-ended tubular cavities by boundary face method. Eng Anal Bound Elem.2013; 37: 542-550.

[24]Wang XH, Zhang JM, Zheng XS, Zhou FL. Half Space Acoustic Problems Analysis by Fast Multipole Boundary Face Method. CMES-Comp Model Eng 2013; 93: 69-90.

[25]Huang C, Zhang JM, Qin XY, Lu CJ, Sheng XM, Li GY. Stress analysis of solids with open-ended tubular holes by BFM. Eng Anal Bound Elem 2012; 3: 1908-1916.

[26]Zhou FL, Zhang JM, Sheng XM, Li GY. A dual reciprocity boundary face method for 3D non-homogeneous elasticity problems. Eng Anal Bound Elem 2012; 36: 1301-1310.

[27]Li GY. Guo SP, Zhang JM, Fei BP, Li Y. Complete solid buckling analysis with Boundary Face Method. CMES-Comp Model Eng 2014; 98: 487-508.

[28] Gaver Jr DP. Observing stochastic processes, and approximate transform inversion. OperRes 1966: 444-459.

[29]Valko PP, Abate J. Comparison of sequence accelerators for the Gaver method of numerical Laplace transform inversion. Comput Math Appl 2004; 48(3-4): 629-636.